AIAA JOURNAL
Vol. 32, No. 4, April 1994

Approach for Simultaneous Optimization of a Structure and Control System

I. Kajiwara,* K. Tsujioka,* and A. Nagamatsu†
Tokyo Institute of Technology, Tokyo 152, Japan

A new approach is presented for simultaneous structural and control optimum design of a system. The design variables of both the structural and the control parameters are optimized simultaneously by the sensitivity analysis to minimize the response due to disturbances of both white noise and colored noise subjected to a constraint so that the system is stable corresponding to high-order natural modes. Three kinds of models are adopted in this approach, namely, the original spatial model by finite element method, the reduced modal model for designing the control system, and the original modal model for assuring stability of the system. The validity and the usefulness of the present approach are verified by a vibration control experiment of a steel plate.

Nomenclature

C_s = $n \times n$ damping matrix of the original FEM model
d = number of disturbances
$E[\cdot]$ = expected value
F = $p \times 2r$ feedback gain matrix
K_s = $n \times n$ stiffness matrix of the original FEM model
M_s = $n \times n$ mass matrix of the original FEM model
n = DOF of the original FEM model
p = number of control inputs
Q = weighting matrix for response
q = state variable vector of the reduced modal model
q_p = state variable vector of the original modal model
q_w = state variable vector of frequency weighting function
R = weighting matrix for control force
r = DOF of the reduced modal model
u = control force vector
v = number of natural modes to be stabilized by optimum design and DOF of the original modal model ($n > v > r$)
w = disturbance vector
x = displacement vector
Λ = $r \times r$ reduced eigenvalue matrix
Λ_e = $v \times v$ original eigenvalue matrix
ξ = reduced modal displacement vector
ξ_e = original modal displacement vector
τ_j = design variable
Φ = $n \times r$ reduced modal matrix
Φ_e = $n \times v$ original modal matrix

Introduction

THE designs of structure and control system are usually carried out separately in machines or mechanical structures that contain control systems. But, with the recent increase in demand for machines having an integrated control system, mutual interaction of the structure and the control system has become an essential factor and plays an important role in the design of them. Especially in vibration control, simultaneous optimum design of the structure and the control system has attracted the attention of engineering researchers in previous decades. Some research has been reported concerning control of flexible structures and simultaneous optimization of the structure and the control system. Salama et al.[1] optimized the structural and the control systems, using a linear combination of two objective functions on the structural and the linear quadratic Gaussian (LQG) control systems. Lim and Junkins[2] optimized the robustness of the control systems, adopting the element of the gain matrix of the output feedback system, the placement of the actuators, and the structural parameters as the design variables. Milman et al.[3] explored the design approach by simultaneous optimization and explained its computational aspects using a simple beam model as an example. Khot and Venkayya[4] provided a method of vibration control of flexible space structures by simultaneously integrating structural design and control design, in which structural modification of a simple truss was performed using the finite element method (FEM) for optimal control by a linear regulator. Venkayya et al.[5] studied structural modeling and optimum control of space structures. Miller et al.[6] examined the structural and control design process of large scale structures by linear regulator theory. Junkins and Rew[7] and Bodden and Junkins[8] proposed an iteration method on optimum structure/control design for preventing vibrations of flexible structures. Haftka et al.[9] discussed two aspects of the sensitivity of a control system to minor structural modifications for combined control/structural design, namely, the sensitivities of the performance and optimum design of the control system. Onoda and Haftka[10] proposed an approach to simultaneous optimum design of a structure and a control system for a large flexible spacecraft. An overview of this research seems to indicate that stability of the system corresponding to high-order natural modes[11] has not been discussed sufficiently in the simultaneous optimum design of the structure and the LQG control system and that experimental verification was not sufficient in previous researches.

The present approach for simultaneous optimization of the structure and the control system assures stability of the system corresponding to high-order natural modes which have been ignored in designing the control system. The disturbances are assumed to be two kinds, namely, a white noise and a colored noise. The original spatial model of the structure of large degrees of freedom (DOF) is made by FEM. Two kinds of modal models are made from this original spatial model. One is the reduced modal model with small DOF of which the control system is composed and optimized. The other is the original modal model of medium DOF used for judging stability of the higher order poles which have been ignored in

Received Feb. 4, 1993; presented as Paper 93-1467 at the AIAA/ASME/ASCE/AHS/ASC 34th Structures, Structural Dynamics, and Materials Conference, La Jolla, CA, April 19–21, 1993; revision received Sept. 24, 1993; accepted for publication Sept. 24, 1993.

*Research Associate, Department of Mechanical Engineering and Science.
†Professor, Department of Mechanical Engineering and Science. Member AIAA.

composing the control system. The structure and the control system are optimized simultaneously to minimize the response under the two constraining conditions: that the control force is smaller than a given value and that the control system is stable corresponding to higher order natural modes. The presented approach has two characteristics. First, this approach is valid in cases where the control system is not only collocative but also noncollocative. Second, it is possible to apply this approach when the disturbance force is not only white noise but also colored noise.

In the present report, first, methods for modeling the structure and for designing the control system are explained. Second, a new approach on simultaneous optimization of the structure and the control system is presented. Third, a method for simultaneous sensitivity analysis is introduced for the linear quadratic Gaussian control system and the FEM structural model. Fourth, the validity and the usefulness of the present method are verified by a vibration control experiment of a steel plate.

Structural Modeling and Design of Control System

The original FEM spatial model of an n DOF structure is explained by the following equation of motion:

$$M_s\ddot{x} + C_s\dot{x} + K_s x = B_{1s}w + B_{2s}u \tag{1}$$

where $M_s, C_s, K_s \in \Re^{n\times n}$ are the mass, the damping, and the stiffness matrices, respectively; and $x \in \Re^n$, $u \in \Re^p$, $w \in \Re^d$ are the displacement, the control force, and the disturbance force vectors, respectively. The damping matrix C_s is neglected in this paper. As n is very large in usual FEM structural models, Eq. (1) cannot be used directly for designing the control system. The following two kinds of modal models are adopted. One is the reduced modal model of r DOF, and the other is the original modal model of v DOF, where $n >> v > r$. The former (r) is used for designing the optimal feedback control system, and the latter (v) is used for assuring stability of this control system corresponding to high natural modes neglected in designing the control system.

Design of Control System with the Reduced Modal Model

Adopting the lower r normalized natural modes $\Phi \in \Re^{n\times r}$, Eq. (1) is transformed to the reduced modal model with the following equation:

$$x = \Phi\xi \tag{2}$$

where $\Phi^T M_s \Phi = I_r$.

The state equation of the reduced modal model becomes

$$\dot{q} = Aq + B_1 w + B_2 u \tag{3}$$

where

$$q = \begin{Bmatrix} \xi \\ \dot{\xi} \end{Bmatrix} \qquad A = \begin{bmatrix} 0 & I_r \\ -\Lambda & 0 \end{bmatrix}$$

$$B_1 = \begin{bmatrix} 0 \\ \Phi^T B_{1s} \end{bmatrix} \qquad B_2 = \begin{bmatrix} 0 \\ \Phi^T B_{2s} \end{bmatrix}$$

The diagonal eigenvalue matrix Λ of this reduced modal model is explained as diag$(\Omega_1^2, \Omega_2^2, \ldots, \Omega_r^2) \in \Re^{r\times r}$, where Ω_i is the ith-order natural frequency ($i = 1 \sim r$).

The spatial output equation is explained as $y = C_0 q_0$, where $C_0 \in \Re^{t\times 2n}$, t is the number of the outputs, and $q_0 = (x^T, \dot{x}^T)^T$. Transforming this output equation from the spatial to the reduced modal coordinates,

$$y = Cq \tag{4}$$

where

$$C = C_0\Psi \qquad \Psi = \begin{bmatrix} \Phi & 0 \\ 0 & \Phi \end{bmatrix}$$

Next, the optimal control system is designed under the assumptions that the system of Eqs. (3) and (4) is both controllable and observable, and that $2r = t$. The restriction $2r = t$ is essential, and it means that DOF of the reduced modal model must be selected always as the half-number of the detected state variables. The feedback gain F is determined by the optimum regulator theory so that the following quadratic performance index which contains both the state variable q and the control force u takes the minimum value:

$$J_q = E[q^T Q q + u^T R u] \tag{5}$$

where Q and R are the weighting matrices. Solving the following algebraic Riccati equation,

$$A^T P + PA + Q - PB_2 R^{-1} B_2^T P = 0 \tag{6}$$

the gain F is obtained as follows:

$$F = R^{-1} B_2^T P \tag{7}$$

The control system is composed of the state feedback control force $u = -Fq$ of the modal coordinates. As $2r = t$, the output matrix C is the square matrix of the rank r, and the state feedback control force of the spatial coordinates is

$$u = -FC^{-1}y \tag{8}$$

This theory allows the design of the noncollocated control system in which the positions of the sensor and of the actuator are different. But, stability of this control system of r DOF is not assured for the natural modes higher than rth. Therefore, this system is optimized to assure this stability, taking the pole arrangement of the closed-loop system of the original modal model into consideration.

Pole Arrangement of Original Modal Model

The normalized natural modes of the number v ($v > r$) are adopted to compose the following original modal model:

$$\dot{q}_e = A_e q_e + B_{1e} w + B_{2e} u \tag{9}$$

where

$$q_e = \begin{Bmatrix} \xi_e \\ \dot{\xi}_e \end{Bmatrix} \qquad A_e = \begin{bmatrix} 0 & I_v \\ -\Lambda_e & 0 \end{bmatrix}$$

$$B_{1e} = \begin{bmatrix} 0 \\ \Phi_e^T B_{1s} \end{bmatrix} \qquad B_{2e} = \begin{bmatrix} 0 \\ \Phi_e^T B_{2s} \end{bmatrix}$$

and $\xi_e \in \Re^v$, the modal matrix $\Phi_e \in \Re^{n\times v}$, the eigenvalue matrix Λ_e = diag$(\Omega_1^2, \Omega_2^2, \ldots, \Omega_v^2) \in \Re^{v\times v}$, and $\Phi_e^T M_s \Phi_e = I_v$.

Using Eq. (8) of the reduced model as the state feedback control force of this original modal model

$$u = -FC^{-1}C_0\Psi_e q_e \tag{10}$$

where

$$\Psi_e = \begin{bmatrix} \Phi_e & 0 \\ 0 & \Phi_e \end{bmatrix}$$

The state equation of the closed-loop system of the original modal model with Eq. (10) is

$$\dot{q}_e = (A_e - B_{2e}FC^{-1}C_0\Psi_e)q_e + B_{1e}w \tag{11}$$

So, the poles s_i ($i = 1 \sim 2\nu$) of this closed-loop system are obtained by eigenvalue analysis of the following equation:

$$G_e = A_e - B_{2e}FC^{-1}C_0\Psi_e \tag{12}$$

As this closed-loop system of the ν DOF is composed of the feedback gain F of the r DOF reduced modal model directly, its stability is not assured for the natural modes higher than the rth one. The stability of the control system is estimated with these poles s_i.

Simultaneous Optimum Design of Structure and Control System

Method of Optimization

A method for optimum design is presented for determining the state feedback gain F to assure stability of the control system of the reduced modal model for all natural modes of the original modal model as well as to optimize the dynamic characteristics of the control system. The following expected values of the square means of the output y and the control force u of the r DOF control system with the reduced modal model are adopted as the cost functions of these dynamic characteristics.

$$H_y = E[y^T\Gamma y] \tag{13}$$

$$H_u = E[u^T\Pi u] \tag{14}$$

where $\Gamma \in \mathcal{R}^{l\times l}$ and $\Pi \in \mathcal{R}^{p\times p}$ are the weighting coefficient matrices. Γ and Π are the constant matrices given beforehand, and quite different from Q and R in Eq. (5). The modal expression of Eq. (13) becomes

$$H_y = E[q^TC^T\Gamma Cq] \tag{15}$$

Equations (13) and (14) are determined as

$$H_y = \mathrm{tr}[P_1B_1VB_1^T] \tag{16}$$

$$H_u = \mathrm{tr}[P_2B_1VB_1^T] \tag{17}$$

where P_1 and P_2 are the solutions of the following Lyapunov equations:

$$P_1G + G^TP_1 + C^T\Gamma C = 0 \tag{18}$$

$$P_2G + G^TP_2 + F^T\Pi F = 0 \tag{19}$$

where

$$G = A - B_2F \tag{20}$$

Equations (18) and (19) are obtained under the assumption that a white noise acts as the disturbance. Next, the cost functions are defined with the expanded state equation in cases where the disturbance is a colored noise f. The state equation becomes, in this case,

$$\dot{q}_w = A_wq_w + B_ww \tag{21}$$

$$f = C_wq_w + D_ww \tag{22}$$

where w is a white noise. The following expanded state equation is introduced with Eqs. (3), (21), and (22):

$$\dot{q}_a = A_aq_a + B_{1a}w + B_{2a}u \tag{23}$$

where

$$q_a = \begin{Bmatrix} q \\ q_w \end{Bmatrix} \qquad A_a = \begin{bmatrix} A & B_1C_w \\ 0 & A_w \end{bmatrix}$$

$$B_{1a} = \begin{bmatrix} B_1D_w \\ B_w \end{bmatrix} \qquad B_{2a} = \begin{bmatrix} B_2 \\ 0 \end{bmatrix}$$

Defining the cost functions of Eqs. (13) and (14) with this expanded state equation, simultaneous optimum design of the structure and control system can be performed according to the given frequency characteristics of the colored noise. The arrangement of the poles of Eq. (11) is taken into consideration in addition to these cost functions to assure stability of the original modal system.

The purpose of optimization is minimization of H_y of Eq. (13) to improve the response. This optimization is performed under the following two constraining conditions. First, H_u of Eq. (14) must be lower than a given positive upper bound $H_u^{\max}$, and the real parts of all poles s_i must be smaller than a given negative upper bound $s_i^{\max}$. Thus, the optimization problem becomes

$$\begin{aligned} &\min H_y \\ &\text{subj} \begin{cases} H_u - H_u^{\max} \le 0 \\ Re(s_i) - s_i^{\max} \le 0 \qquad (i = 1 \sim 2\nu) \end{cases} \end{aligned} \tag{24}$$

Dynamic response, control force, and stability are taken as the factors for optimization in the objective function and the constraining conditions of Eq. (24) in this paper. But it is not difficult to generalize the concept of optimum design, taking into account the other factors additionally, such as weight, stress, or cost.

The optimal values of the design variables are determined according to Eq. (24), using the nonlinear optimization method with the quasi-Newton method and the Lagrangean multiplier

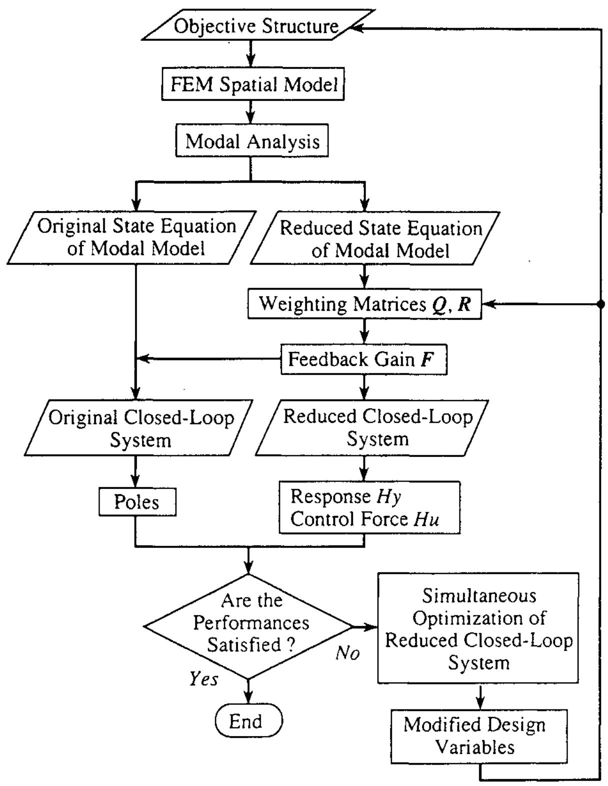

Fig. 1 Flow chart of the proposed method.

method. The overall flow chart of this approach is shown in Fig. 1.

Based on the present method of simultaneous optimizations, no tradeoff relations exist between the structural and control optimizations.

Definition of Design Variables

In the present report, the thickness of the plate is taken as the design variables of the structure, and the elements of the weighting matrices $\boldsymbol{Q}$ and $\boldsymbol{R}$ in Eq. (5) are taken as the design variables of the control system. Allowable changes of the structural variables are often limited in actual design, for example $t_{\min} \le t_i \le t_{\max}$ in this paper. To take this limit into the optimization procedure in advance, the thickness of the plate t_i is defined with the following function of the design variable α_i:

$$t_i = \frac{t_{\max} - t_{\min}}{1 + \exp\{-\alpha_i\}} + t_{\min}, \qquad (-\infty \le \alpha_i \le \infty) \tag{25}$$

where $t_{\max}$ and $t_{\min}$ are the upper and the lower limits of change of t_i, respectively. To keep the positive-definite condition, $\boldsymbol{Q}$ and $\boldsymbol{R}$ are transformed by Cholesky decomposition as

$$\boldsymbol{Q} = \boldsymbol{L}^T\boldsymbol{L} \tag{26}$$

$$\boldsymbol{R} = \boldsymbol{U}^T\boldsymbol{U} \tag{27}$$

and $\boldsymbol{L}$ and $\boldsymbol{U}$ are taken as the design variables instead of $\boldsymbol{Q}$ and $\boldsymbol{R}$.

Sensitivity Analysis

Sensitivity of Quadratic Cost Function

The design variables of the structure and the control system are defined as τ_j collectively. Partially differentiating Eqs. (16) and (17) with respect to τ_j, the sensitivities of H_y and H_u defined with Eqs. (13) and (14) are

$$\frac{\partial H_y}{\partial \tau_j} = \mathrm{tr}\left[\frac{\partial \boldsymbol{P}_1}{\partial \tau_j}\boldsymbol{B}_1\boldsymbol{V}\boldsymbol{B}_1^T + \boldsymbol{P}_1\frac{\partial \boldsymbol{B}_1}{\partial \tau_j}\boldsymbol{V}\boldsymbol{B}_1^T + \boldsymbol{P}_1\boldsymbol{B}_1\boldsymbol{V}\frac{\partial \boldsymbol{B}_1^T}{\partial \tau_j}\right] \tag{28}$$

$$\frac{\partial H_u}{\partial \tau_j} = \mathrm{tr}\left[\frac{\partial \boldsymbol{P}_2}{\partial \tau_j}\boldsymbol{B}_1\boldsymbol{V}\boldsymbol{B}_1^T + \boldsymbol{P}_2\frac{\partial \boldsymbol{B}_1}{\partial \tau_j}\boldsymbol{V}\boldsymbol{B}_1^T + \boldsymbol{P}_2\boldsymbol{B}_1\boldsymbol{V}\frac{\partial \boldsymbol{B}_1^T}{\partial \tau_j}\right] \tag{29}$$

The sensitivities of $\boldsymbol{P}_1$ and $\boldsymbol{P}_2$ are obtained, solving the following equations which are partial differentiations of Eqs. (18) and (19):

$$\frac{\partial \boldsymbol{P}_1}{\partial \tau_j}\boldsymbol{G} + \boldsymbol{G}^T\frac{\partial \boldsymbol{P}_1}{\partial \tau_j} + \boldsymbol{P}_1\frac{\partial \boldsymbol{G}}{\partial \tau_j} + \frac{\partial \boldsymbol{G}^T}{\partial \tau_j}\boldsymbol{P}_1 + \frac{\partial \boldsymbol{C}^T}{\partial \tau_j}\boldsymbol{\Gamma}\boldsymbol{C} + \boldsymbol{C}^T\boldsymbol{\Gamma}\frac{\partial \boldsymbol{C}}{\partial \tau_j} = \boldsymbol{0} \tag{30}$$

$$\frac{\partial \boldsymbol{P}_2}{\partial \tau_j}\boldsymbol{G} + \boldsymbol{G}^T\frac{\partial \boldsymbol{P}_2}{\partial \tau_j} + \boldsymbol{P}_2\frac{\partial \boldsymbol{G}}{\partial \tau_j} + \frac{\partial \boldsymbol{G}^T}{\partial \tau_j}\boldsymbol{P}_2 + \frac{\partial \boldsymbol{F}^T}{\partial \tau_j}\boldsymbol{\Pi}\boldsymbol{F} + \boldsymbol{F}^T\boldsymbol{\Pi}\frac{\partial \boldsymbol{F}}{\partial \tau_j} = \boldsymbol{0} \tag{31}$$

Equations (20), (7), and (6) are differentiated partially as follows to obtain the sensitivities of $\boldsymbol{G}$ and $\boldsymbol{F}$:

$$\frac{\partial \boldsymbol{G}}{\partial \tau_j} = \frac{\partial \boldsymbol{A}}{\partial \tau_j} - \frac{\partial \boldsymbol{B}_2}{\partial \tau_j}\boldsymbol{F} - \boldsymbol{B}_2\frac{\partial \boldsymbol{F}}{\partial \tau_j} \tag{32}$$

$$\frac{\partial \boldsymbol{F}}{\partial \tau_j} = -\boldsymbol{R}^{-1}\frac{\partial \boldsymbol{R}}{\partial \tau_j}\boldsymbol{R}^{-1}\boldsymbol{B}_2^T\boldsymbol{P} + \boldsymbol{R}^{-1}\frac{\partial \boldsymbol{B}_2^T}{\partial \tau_j}\boldsymbol{P} + \boldsymbol{R}^{-1}\boldsymbol{B}_2^T\frac{\partial \boldsymbol{P}}{\partial \tau_j} \tag{33}$$

$$\boldsymbol{G}^T\frac{\partial \boldsymbol{P}}{\partial \tau_j} + \frac{\partial \boldsymbol{P}}{\partial \tau_j}\boldsymbol{G} + \left(\frac{\partial \boldsymbol{A}^T}{\partial \tau_j}\boldsymbol{P} + \boldsymbol{P}\frac{\partial \boldsymbol{A}}{\partial \tau_j} + \frac{\partial \boldsymbol{Q}}{\partial \tau_j} - \boldsymbol{P}\frac{\partial \boldsymbol{B}_2}{\partial \tau_j}\boldsymbol{F} - \boldsymbol{F}^T\frac{\partial \boldsymbol{B}_2^T}{\partial \tau_j}\boldsymbol{P} + \boldsymbol{F}^T\frac{\partial \boldsymbol{R}}{\partial \tau_j}\boldsymbol{F}\right) = \boldsymbol{0} \tag{34}$$

The sensitivity of $\boldsymbol{P}$ is obtained by solving Eq. (34).

Sensitivity of Pole of Original Modal System

The Laplace transform of Eq. (11) is

$$(s\boldsymbol{I}_{2\nu} - \boldsymbol{G}_e)\boldsymbol{q}_e(s) = \boldsymbol{B}_{1e}\boldsymbol{w}(s) \tag{35}$$

The poles s_i and the right eigenvectors $\boldsymbol{\phi}_{iR}$ $(i = 1 \sim 2\nu)$ are given as the solutions of the eigenvalue analysis of Eq. (35), the right-hand side of which is replaced by zero. Substituting these eigenpairs into Eq. (35) and partially differentiating the resultant equation we have

$$\left(\frac{\partial s_i}{\partial \tau_j}\boldsymbol{I}_{2\nu} - \frac{\partial \boldsymbol{G}_e}{\partial \tau_j}\right)\boldsymbol{\phi}_{iR} + (s\boldsymbol{I}_{2\nu} - \boldsymbol{G}_e)\frac{\partial \boldsymbol{\phi}_{iR}}{\partial \tau_j} = 0 \tag{36}$$

Partially differentiating Eq. (12), the sensitivity of $\boldsymbol{G}_e$ is obtained as follows:

$$\frac{\partial \boldsymbol{G}_e}{\partial \tau_j} = \frac{\partial \boldsymbol{A}_e}{\partial \tau_j} - \frac{\partial \boldsymbol{B}_{2e}}{\partial \tau_j}\boldsymbol{F}\boldsymbol{C}^{-1}\boldsymbol{C}_0\boldsymbol{\Psi}_e - \boldsymbol{B}_{2e}\frac{\partial \boldsymbol{F}}{\partial \tau_j}\boldsymbol{C}^{-1}\boldsymbol{C}_0\boldsymbol{\Psi}_e + \boldsymbol{B}_{2e}\boldsymbol{F}\boldsymbol{C}^{-1}\frac{\partial \boldsymbol{C}}{\partial \tau_j}\boldsymbol{C}^{-1}\boldsymbol{C}_0\boldsymbol{\Psi}_e - \boldsymbol{B}_{2e}\boldsymbol{F}\boldsymbol{C}^{-1}\boldsymbol{C}_0\frac{\partial \boldsymbol{\Psi}_e}{\partial \tau_j} \tag{37}$$

where the sensitivity of $\boldsymbol{F}$ is given as Eq. (33). Multiplying the left eigenvector $\boldsymbol{\phi}_{iL}^T$ to Eq. (36) from the left-hand side, the second term on the left side of the resultant equation vanishes, and the sensitivity of the pole s_i is

$$\frac{\partial s_i}{\partial \tau_j} = \frac{\boldsymbol{\phi}_{iL}^T(\partial \boldsymbol{G}_e/\partial \tau_j)\boldsymbol{\phi}_{iR}}{\boldsymbol{\phi}_{iL}^T\boldsymbol{\phi}_{iR}} \tag{38}$$

To calculate the given sensitivities, the sensitivities of the matrices $\boldsymbol{A}$, $\boldsymbol{B}_1$, $\boldsymbol{B}_2$, $\boldsymbol{C}$, $\boldsymbol{A}_e$, and $\boldsymbol{B}_{2e}$ which are contained in the state equation, and of the matrices $\boldsymbol{L}$ and $\boldsymbol{U}$ which are contained in the cost function, must be calculated beforehand. In the case of colored noise, the matrices $\boldsymbol{A}$, $\boldsymbol{B}_1$, and $\boldsymbol{B}_2$ in the preceding series of equations are replaced with the given matrices $\boldsymbol{A}_a$, $\boldsymbol{B}_{1a}$, and $\boldsymbol{B}_{2a}$, respectively.

Sensitivity with Respect to Structural Design Variable

The sensitivity of the arbitrary function H concerning the structural design variable α_i is found from Eq. (25) as follows:

$$\frac{\partial H}{\partial \alpha_j} = \frac{\partial H}{\partial t_j}\frac{\partial t_j}{\partial \alpha_j} \tag{39}$$

Since $\partial t_i/\partial \alpha_i$ in Eq. (39) is obtained easily from Eq. (25), only $\partial H/\partial t_i$ is necessary for calculating the sensitivity with Eq. (39). It is obvious from Eqs. (3) and (9) that the sensitivities of the matrices $\boldsymbol{A}$, $\boldsymbol{B}_1$, $\boldsymbol{B}_2$, $\boldsymbol{C}$, $\boldsymbol{A}_e$, and $\boldsymbol{B}_{2e}$ can be calculated, only if the sensitivities of the eigenvalue matrix $\boldsymbol{\Lambda}_e$ and the natural mode matrix $\boldsymbol{\Phi}_e$ are known. On the other hand, the sensitivities of $\boldsymbol{L}$ and $\boldsymbol{U}$ do not exist in the case of structural design variables.

The sensitivity of the eigenvalue Ω_i with respect to the thickness of the plate is

$$\frac{\partial \Omega_i}{\partial t_j} = \frac{\boldsymbol{\phi}_i^T(\partial \boldsymbol{K}_s/\partial t_j - \Omega_i^2\partial \boldsymbol{M}_s/\partial t_j)\boldsymbol{\phi}_i}{2\Omega_i} \tag{40}$$

The sensitivity of the natural mode $\boldsymbol{\phi}_i$ is

$$\frac{\partial \boldsymbol{\phi}_i}{\partial t_j} = \boldsymbol{\Phi}_m\boldsymbol{\eta} \tag{41}$$

where $\boldsymbol{\Phi}_m \in \Re^{n \times m}(m > \nu)$ is the modal matrix. The component η_k of the modal coordinates $\boldsymbol{\eta} \in \Re^m$ is obtained with the following equation:

$$\eta_k = -\frac{1}{\Omega_k^2 - \Omega_i^2} \boldsymbol{\phi}_k^T \left(\frac{\partial \boldsymbol{K}_s}{\partial t_j} - \Omega_i^2 \frac{\partial \boldsymbol{M}_s}{\partial t_j} \right) \boldsymbol{\phi}_i \qquad (k \neq i) \tag{42}$$

$$\eta_i = -\boldsymbol{\phi}_i^T \frac{\partial \boldsymbol{M}_s}{\partial t_j} \boldsymbol{\phi}_i / 2 \tag{43}$$

Equations (40), (42), and (43) denote that the sensitivities of the mass matrix $\boldsymbol{M}_s$ and the stiffness matrix $\boldsymbol{K}_s$ are necessary for calculating the sensitivities of the eigenvalue and the natural mode. In the case of FEM, the sensitivity of $\boldsymbol{M}_s$ is obtained with the following surface integration over the finite elements which are optimized:

$$\frac{\partial \boldsymbol{M}_s}{\partial t_j} = \rho \int_S \boldsymbol{N}^T \boldsymbol{N} \, \mathrm{d}S \tag{44}$$

where ρ is the density of the material and $\boldsymbol{N}$ the shape function. The sensitivities of the stiffness matrix $\boldsymbol{K}_p$ in in-plane deformation and the stiffness matrix $\boldsymbol{K}_l$ in out-of-plane deformation are given as

$$\frac{\partial \boldsymbol{K}_p}{\partial t_j} = \frac{E_y}{1 - \nu^2} \int_S \boldsymbol{D}^T \boldsymbol{E}_s \boldsymbol{D} \, \mathrm{d}S \tag{45}$$

$$\frac{\partial \boldsymbol{K}_l}{\partial t_j} = \frac{t_j^2 E_y}{4(1 - \nu^2)} \int_S \boldsymbol{D}^T \boldsymbol{E}_s \boldsymbol{D} \, \mathrm{d}S \tag{46}$$

where ν is Poisson's ratio and E_y Young's modulus. $\boldsymbol{D}$ and $\boldsymbol{E}_s$ are the matrices which explain the strain-deformation and the strain-stress relationships, respectively.

Sensitivity with Respect to Design Variable of Control System

The sensitivity matrices of $\boldsymbol{L}$ and $\boldsymbol{U}$ are defined as $\partial \boldsymbol{L}/\partial L_{i,j}$ and $\partial \boldsymbol{U}/\partial U_{i,j}$, in which the i, j elements are unity and all other elements are zero. So, the sensitivities of $\boldsymbol{L}$ and $\boldsymbol{Q}$ are obtained very easily. On the other hand, the sensitivities of $\boldsymbol{A}$, $\boldsymbol{B}_1$, $\boldsymbol{B}_2$, $\boldsymbol{C}$, $\boldsymbol{A}_e$, and $\boldsymbol{B}_{2e}$ do not exist in this case.

Experimental Verification

A rectangular plate of stainless steel with a fixed end shown in Fig. 2, is taken as the object structure, and its vibration is suppressed with the control system designed by the method presented in this report. The initial thickness of this plate is 4 mm. This plate is divided into 80 nodal points and 64 elements to make the FEM model. The displacement in the normal direction to the surface is measured at two points (24 and 66) with two gap sensors. The detected signals are fed into the digital signal processor (DSP32C from AT&T) after analog to digital (A/D) transformation, and necessary computation for control is performed with the sampling frequency of 15 kHz. After digital to analog (D/A) transformation, the output signals are fed to two voice coil actuators attached at the points 19 and 72 on the surface of the plate to generate the control force. The white noise or the colored noise is input at the point 72. Thus, the output and the control force vectors are as follows:

$$\boldsymbol{y} = (y_{24}, y_{66}, \dot{y}_{24}, \dot{y}_{66})^T \tag{47}$$

$$\boldsymbol{u} = (u_{19}, u_{72})^T \tag{48}$$

Thus, the relation of collocation does not exist in this control system.

The frequency response function (FRF) between the disturbance at the point 72 and the output at the point 66 when the control system does not act is shown in Fig. 3 as the ratio of the disturbance force voltage which acts on the voice coil

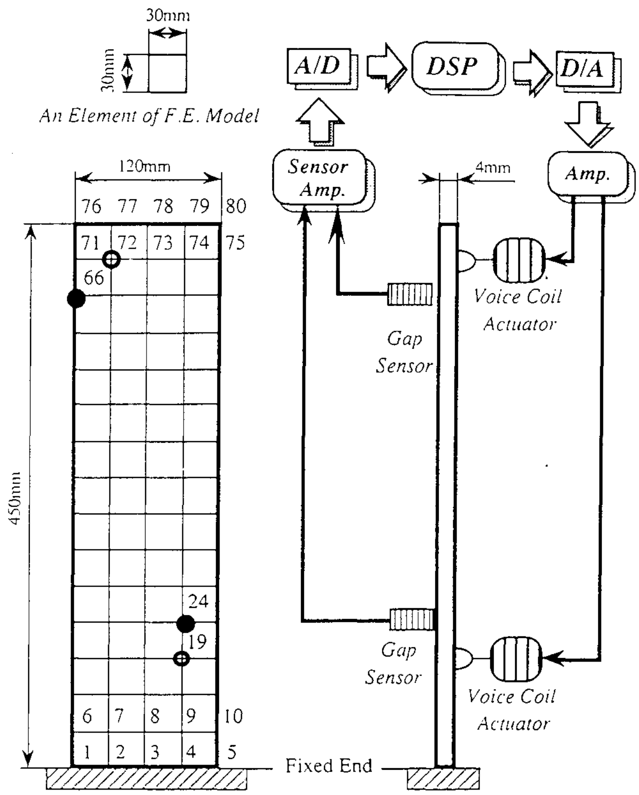

Fig. 2 Experimental setup.

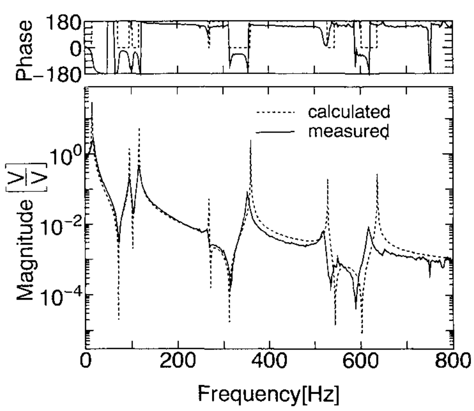

Fig. 3 FRF without control.

actuator to the detected displacement voltage with the gap sensor. The experimental result (the solid line) agrees well with the calculated one (the dotted line) in Fig. 3, and seven resonance peaks are found in the frequency region lower than 800 Hz.

The control system is composed with a 2-DOF reduced modal model using the first and the second natural modes. Simultaneous optimum design of this 2-DOF control system and the plate thickness is performed to assure stability of this control system corresponding to these seven natural modes.

White Noise Disturbance

First, optimum design of only the control system is done, adopting the first column elements of the weighting matrix $\boldsymbol{L}$ of Eq. (26) as the design variables. The weighting coefficient matrices in Eqs. (13) and (14) are given as $\boldsymbol{\Gamma} = \mathrm{diag}(1, 1, 0, 0)$ and $\boldsymbol{\Pi} = \mathrm{diag}(1, 1)$, respectively. The quadratic performance indices on the output signal and the control force are as follows:

$$H_y = E[y_{24}^2 + y_{66}^2] \tag{49}$$

$$H_u = E[u_{19}^2 + u_{72}^2] \tag{50}$$

The initial weighting matrices in Eqs. (26) and (27) are given as

$$L = \begin{bmatrix} 1 & 1 & 1 & 0.1 \\ 0 & 0 & 0 & 0 \\ 0 & 0 & 0 & 0 \\ 0 & 0 & 0 & 0 \end{bmatrix} \qquad U = \begin{bmatrix} 1 & 0 \\ 0 & 1 \end{bmatrix} \tag{51}$$

Thus, the initial values of H_y and H_u in Eqs. (49) and (50) become $H_y^{\text{org}} = 4.11$ and $H_u^{\text{org}} = 23.7$, respectively, when the disturbance force of intensity $V = 1$ acts on point 72. The initial poles of the closed-loop system under these conditions are shown as the square points in Fig. 4, and the sixth pole becomes unstable.

The optimum control system design is performed under the conditions that the upper bounds of the constraining conditions on the control force and the poles are

$$H_u^{\max} = 70 \qquad s_i^{\max} = -3 \quad (\forall i) \tag{52}$$

As the result, the optimum weighting matrix L becomes

$$L_c^{\text{opt}} = \begin{bmatrix} 11.56 & 10.33 & 2.380 & 1.083 \\ 0 & 0 & 0 & 0 \\ 0 & 0 & 0 & 0 \\ 0 & 0 & 0 & 0 \end{bmatrix} \tag{53}$$

The optimum value of the objective function becomes $H_y^{\text{opt}} = 1.63$, and the optimum value on the control force takes the upper bound as $H_u^{\text{opt}} = 70.0$. The optimum poles become stable as shown as the open circles in Fig. 4. FRF between the disturbance w_{72} and the output y_{66} is shown in Fig. 5,

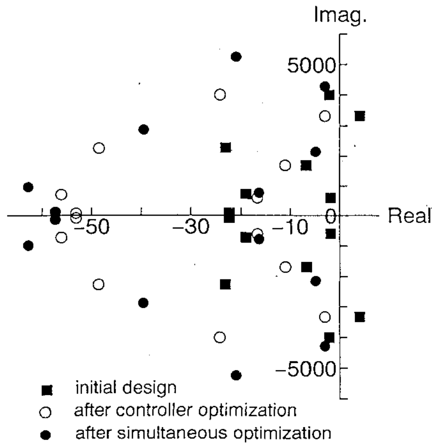

Fig. 4 Pole plots of the closed-loop system.

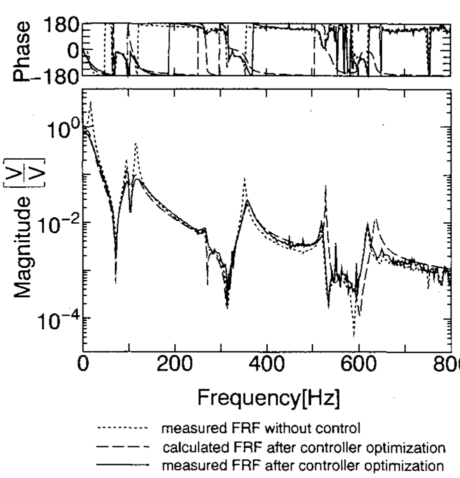

Fig. 5 FRF of nominal structure by control system optimization.

where the dotted line is the experimental result without control, the broken line is the calculated result with optimal control, and the solid line is the experimental result with optimal control. Figure 5 indicates that the response levels decrease at the resonance peaks by optimum control.

Next, simultaneous optimum design is performed, adopting the weighting matrix L with the thicknesses of the plate at five regions as shown in Fig. 6 as the design variables. The bounds of the allowable thicknesses t_i ($i = 1 \sim 5$) in Eq. (25) are given as

$$3 \le t_i \le 6.5 \tag{54}$$

The upper bounds of H_u and s_i are given as in Eq. (52).

As the result of simultaneous optimum design by the method presented in this report, the optimum weighting matrix L becomes

$$L_{s1}^{\text{opt}} = \begin{bmatrix} 0.9795 & 1.066 & 2.788 & 1.081 \\ 0 & 0 & 0 & 0 \\ 0 & 0 & 0 & 0 \\ 0 & 0 & 0 & 0 \end{bmatrix} \tag{55}$$

The optimum values of the thicknesses of the plate are shown in Table 1. The optimum value of the object function is $H_y^{\text{opt}} = 0.484$, and the performance index of the control force is $H_u^{\text{opt}} = 70.0$. The object function in this case becomes smaller than that in the earlier case of the control system optimization. The poles in the case of simultaneous optimization are shown as the solid circles in Fig. 4. FRF between w_{72} and y_{66} is shown in Fig. 7 in which the dotted line is the experimental result on the nominal structure in the case of the control system optimization, and the broken and the solid lines are the calculated and the experimental results, respectively, in the case of simultaneous optimization. The time history of the experimental result of the response at the point 66 when a white noise disturbance acts at the point 72 is shown in Fig. 8 in which the dotted line is the case of optimizing only the control system, and the solid line is the case of simultaneous optimization. Figures 7 and 8 show that the response becomes

Table 1 Optimal values of plate thickness

Region no.	1	2	3	4	5
Thickness, mm	5.89	5.37	4.94	4.54	5.35

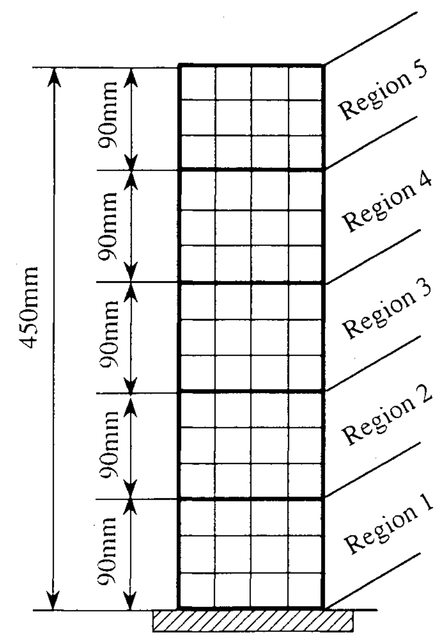

Fig. 6 Regions of design variable.

Table 2 Optimal values of plate thickness

Region no.	1	2	3	4	5
Thickness, mm	6.49	5.57	6.46	6.48	5.67

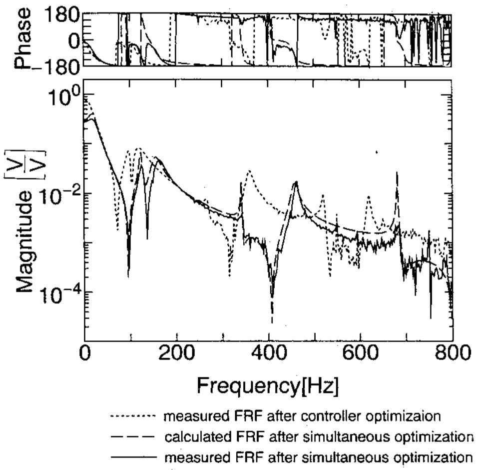

Fig. 7 FRF after simultaneous optimization.

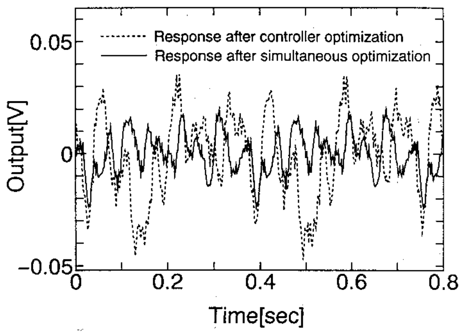

Fig. 8 Response with white noise disturbance.

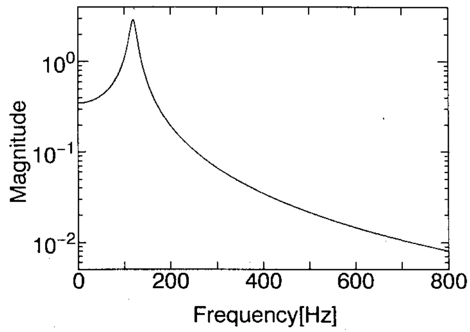

Fig. 9 Frequency spectrum of the colored disturbance.

smaller in simultaneous optimization than in control system optimization.

Colored Noise Disturbance

Figure 7 shows that 120 Hz is near the third resonance peak in the case of the control system optimization and near the second resonance peak in the case of simultaneous optimization. Here, it is assumed that a colored noise which has a dominant component at 120 Hz, as shown in Fig. 9, acts as the disturbance force. The simultaneous optimization is performed in this case with the expanded state equations (21–23), taking the thicknesses in Table 1 and the matrix in Eq. (55) as the initial values of the design variables, which are the results of the previous simultaneous optimization. The initial values of H_y and H_u are calculated with Eq. (23) as $H_y^{\mathrm{org}} = 0.113$ and $H_u^{\mathrm{org}} = 80.2$. All bounds of the design variables are same as the previous case of white noise. H_y is

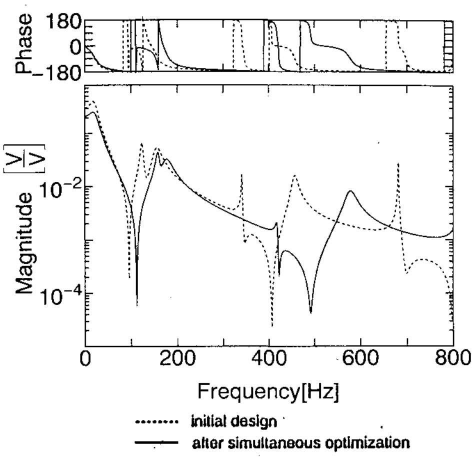

Fig. 10 FRF after simultaneous optimization.

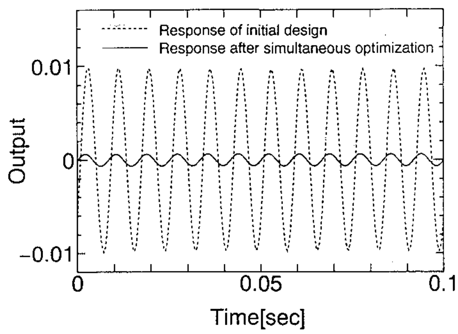

Fig. 11 Response when harmonic disturbance acts.

taken as the object function, and the constraint conditions are given as

$$H_u^{\max} = 20.0 \qquad s_i^{\max} = -3 \qquad (\forall i) \tag{56}$$

As the result of simultaneous optimization, the optimal value of the matrix $\boldsymbol{L}$ becomes

$$\boldsymbol{L}_{s2}^{\mathrm{opt}} = \begin{bmatrix} 0.9802 & 1.068 & 3.859 & 1.866 \\ 0 & 0 & 0 & 0 \\ 0 & 0 & 0 & 0 \\ 0 & 0 & 0 & 0 \end{bmatrix} \tag{57}$$

and the optimal values of the thicknesses of the plate are shown in Table 2. The optimal value of the objective function becomes $H_y^{\mathrm{opt}} = 0.0319$, and the optimal value of H_u becomes $H_u^{\mathrm{opt}} = 20.0$. The calculated result of FRF between w_{72} and y_{66} is shown in Fig. 10 in which the dotted line is the case of the initial control, and the solid line is the case of control after simultaneous optimization. Figure 10 shows that the initial resonance peak near 120 Hz moves to another frequency, and the response level near 120 Hz decreases significantly after simultaneous optimization. The calculated result of the response at point 66 when a harmonic disturbance of 120 Hz acts at the point 72 is shown in Fig. 11 in which the dotted line is the case of initial control, and the solid line is the case of control after simultaneous optimization. The solid line is much smaller than the dotted line in Fig. 11. Thus, simultaneous optimization of the structural and the control systems is especially efficient and useful in cases when the colored noise acts as the disturbance.

Conclusions

1) A new approach for simultaneous optimum design of the structure and the control system is presented to suppress the vibration of a mechanical structure most efficiently and to assure stability of the system corresponding to some of the

higher order natural modes which are ignored in designing the control system.

2) Effective vibration control performances are obtained by the present approach when the disturbances of not only white noise but also colored noise act on the system.

3) The present approach is effective for a noncollocation control system.

4) Good agreement of the experimental results with the calculated results proves the validity and the effectiveness of the present approach.

References

[1]Salama, M., Garba, J., and Demsetz, L., "Simultaneous Optimization of Controlled Structures," *Computational Mechanics*, Vol. 3, No. 4, 1988, pp. 275–282.

[2]Lim, K. B., and Junkins, J. L., "Robustness Optimization of Structural and Controller Parameters," *Journal of Guidance, Control, and Dynamics*, Vol. 12, No. 1, 1989, pp. 89–96.

[3]Milman, M., Salama, M., Scheid, R. E., Bruno, R., and Gibson, J. S., "Combined Control-Structural Optimization," *Computational Mechanics*, Vol. 8, No. 1, 1991, pp. 1–18.

[4]Khot, N. S., and Venkayya, V. B., "Optimal Structural Modifications to Enhance the Active Vibration Control of Flexible Structures," *AIAA Journal*, Vol. 24, No. 8, 1986, pp. 1368–1374.

[5]Venkayya, V. B., Tischler, V. A., and Khot, N. S., "Dynamics and Control of Space Structure," *Engineering Optimization*, Vol. 11, Nos. 3/4, 1987, pp. 251–264.

[6]Miller, D. F., Venkayya, V. B., and Tischler, V. A., "Integration of Structures and Controls. Some Computational Issues," *Proceedings of the 24th IEEE Conference on Decision and Control*, Vol. 2, Dec. 1985, pp. 924–931.

[7]Junkins, J. L., and Rew, D. W., "A Simultaneous Structure/Controller Design Iteration Method," *IEEE Proceedings of the 1985 American Control Conference*, Vol. 3, June 1985, pp. 1642–1647.

[8]Bodden, D. S., and Junkins, J. L., "Eigenvalue Optimization Algorithms for Structure/Controller Design Iterations," *Journal of Guidance, Control, and Dynamics*, Vol. 8, No. 6, 1985, pp. 697–706.

[9]Haftka, R. T., Martinovic, Z. N., Hallauer, W. L., Jr., and Schamel, G., "An Analytical and Experimental Study of a Control System's Sensitivity to Structural Modifications," *AIAA Journal*, Vol. 25, No. 2, 1987, pp. 310–315.

[10]Onoda, J., and Haftka, R. T., "An Approach to Structure/Control Simultaneous Optimization for Large Flexible Spacecraft," *AIAA Journal*, Vol. 25, No. 8, 1987, pp. 1133–1138.

[11]Kajiwara, I., and Nagamatsu, A., "Optimum Design of Control System for Large Degrees-of-Freedom Structure to Assure Stability Against High Mode Vibrational Disturbance," *AIAA/ASME/ASCE/AHS/ASC 33rd Structures, Structural Dynamics, and Materials Conference,* Dallas, TX, April 1992, pp. 1595-1603; also AIAA Paper 92-2323.